

Article

## Shark Variable New Antigen Receptor ( $V_{\text{NAR}}$ ) Single Domain Antibody Fragments: Stability and Diagnostic Applications

Katherine Griffiths<sup>1,2</sup>, Olan Dolezal<sup>3</sup>, Kathy Parisi<sup>1,2</sup>, Julie Angerosa<sup>3</sup>, Con Dogovski<sup>1</sup>, Miles Barraclough<sup>3</sup>, Abdulmonem Sanalla<sup>1,2</sup>, Joanne L. Casey<sup>1</sup>, Iveth González<sup>4</sup>, Matthew A. Perugini<sup>1</sup>, Stewart Nuttall<sup>3</sup> and Michael Foley<sup>1,2,\*</sup>

<sup>1</sup> The Department of Biochemistry, La Trobe Institute for Molecular Science, La Trobe University, Plenty Road, Bundoora, VIC., 3086, Australia

<sup>2</sup> AdAlta Pty. Ltd., 15/2 Park Drive, Bundoora, VIC., 3086, Australia

<sup>3</sup> The CSIRO Materials Science and Engineering, 343 Royal Parade, Parkville, VIC., 3052, Australia

<sup>4</sup> The Foundation for Innovative New Diagnostics (FIND), Avenue de Budé 16, 1202 Geneva, Switzerland

\* Author to whom correspondence should be addressed; E-Mail: M.Foley@latrobe.edu.au; Tel.: +613-94792158.

Received: 29 November 2012; in revised form: 9 January 2013 / Accepted: 21 January 2013 /

Published: 25 January 2013

---

**Abstract:** The single variable new antigen receptor domain antibody fragments ( $V_{\text{NARS}}$ ) derived from shark immunoglobulin new antigen receptor antibodies (IgNARs) represent some of the smallest known immunoglobulin-based protein scaffolds. As single domains, they demonstrate favorable size and cryptic epitope recognition properties, making them attractive in diagnosis and therapy of numerous disease states. Here, we examine the stability of  $V_{\text{NAR}}$  domains with a focus on a family of  $V_{\text{NARS}}$  specific for apical membrane antigen 1 (AMA-1) from *Plasmodium falciparum*. The  $V_{\text{NARS}}$  are compared to traditional monoclonal antibodies (mAbs) in liquid, lyophilized and immobilized nitrocellulose formats. When maintained in various formats at 45 °C,  $V_{\text{NARS}}$  have improved stability compared to mAbs for periods of up to four weeks. Using circular dichroism spectroscopy we demonstrate that  $V_{\text{NAR}}$  domains are able to refold following heating to 80 °C. We also demonstrate that  $V_{\text{NAR}}$  domains are stable during incubation under potential *in vivo* conditions such as stomach acid, but not to the protease rich environment of murine stomach scrapings. Taken together, our results demonstrate the suitability of shark  $V_{\text{NAR}}$  domains for various diagnostic platforms and related applications.

**Keywords:** single-domain antibody; shark  $V_{\text{NAR}}$ ; thermal stability; pH stability; protease resistance; AMA-1; *Plasmodium*; malaria; diagnosis

---

## 1. Introduction

The development of rapid, accurate and low cost diagnostics for point-of-care applications in developing countries is a major challenge that needs to be overcome if the morbidity and mortality from diseases is to be reduced in these countries. Such diagnostic tests must be easy to use and sufficiently robust to survive exposure to extremes of temperature and humidity. Many of the rapid diagnostic tests currently in use rely on conventional murine-derived antibodies for the detection of pathogens or molecules derived from them. Monoclonal antibodies (mAbs) have a variety of features that make them particularly well suited to this task, such as high specificity and high affinity for the target antigen. However, despite these favorable characteristics, diagnostic tests based upon such antibodies may be adversely affected by high temperatures or by storage for extended periods under conditions of high humidity, particularly when the test must be conducted in developing countries where constant access to refrigeration is not always practicable [1].

Over the last 15 years, technologies based upon the immunoglobulin new antigen receptor (IgNAR) class of antibodies from the shark immune repertoire have been developed that can potentially overcome mAb limitations. Mature IgNAR antibodies consist of homodimers of one variable new antigen receptor ( $V_{\text{NAR}}$ ) domain and five constant new antigen receptor ( $C_{\text{NAR}}$ ) domains [2]. The evolution of IgNARs to a single domain conformation over significant periods of evolutionary time has resulted in molecules that are highly stable and possess efficient binding characteristics. The inherent stability can be attributed to both (i) the underlying Ig scaffold, which presents a considerable number of charged and hydrophilic surface exposed residues compared to the conventional antibody  $V_{\text{H}}$  and  $V_{\text{L}}$  domains found in murine antibodies; and (ii) stabilizing structural features in the complementary determining region (CDR) loops including inter-loop disulphide bridges, and patterns of intra-loop hydrogen bonds [3,4].

As a consequence, we hypothesized that individual  $V_{\text{NAR}}$  domains would display high stability under conditions that would otherwise compromise the integrity of traditional monoclonal antibodies. Such stability, if demonstrable as a consistent feature of these binding reagents, would be advantageous for use in diagnostic assays where the reagents are likely to be exposed to extreme conditions.

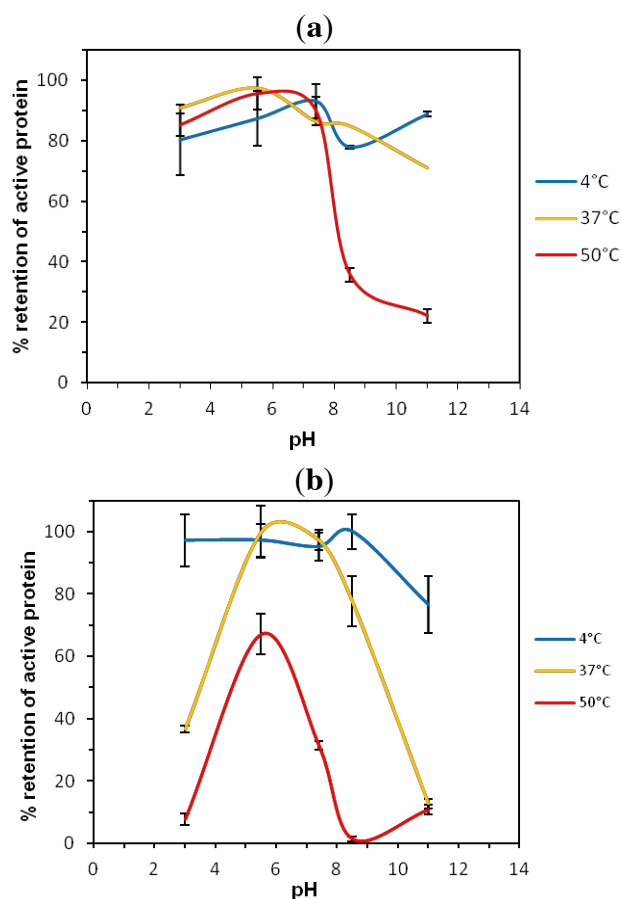
Over recent years, we have developed in particular a model system based around the 12Y-2 family of  $V_{\text{NARS}}$  that target the apical membrane antigen 1 (AMA-1) of malarial (*Plasmodium falciparum*) parasites [5]. Studies have included  $V_{\text{NAR}}$  affinity maturation [6], structural studies [3], multimerisation strategies [7], library design and selection to enhance cross-strain binding [8]. Here, we utilize several of these AMA-1  $V_{\text{NARS}}$  along with a model  $V_{\text{NAR}}$  to illustrate stability properties of the scaffold in conditions including extreme temperature and pH and in the presence of proteases. We have consequently identified a set of conditions which allows one  $V_{\text{NAR}}$  to retain significant activity for up to 4 weeks at 50 °C.

## 2. Results and Discussion

### 2.1. Thermostability of $V_{NARS}$ at Extreme pH

The  $V_{NAR}$  4A-1 binds to a mAb antigen, 5G8, with an affinity of 1  $\mu$ M (Appendix Figure A1). The paratope of the antibody is readily targeted by our single domain  $V_{NAR}$  variants via the motif S/AYP [9]. The 4A-1 variant is hence regarded as a model  $V_{NAR}$ . Thermostability experiments were conducted to examine the stability of this  $V_{NAR}$  in liquid format at various pH values and temperatures. ProteOn XPR36 SPR biosensor was utilized for the determination of residual binding activities of 4A-1. After 1 day incubation at 4, 37 or 50 °C there was a trend for greater retention of activity at pHs  $\leq 7.4$  (Figure 1a). At 4 °C or 37 °C retention of active protein was 90% and 70%, respectively, whereas after incubation at 50 °C, only 20% active protein was retained. After 4 weeks incubation at 4 °C retention of active protein was  $\geq 70\%$  at all pH values investigated (Figure 1b). At 37 °C, retention of active protein was 100% at pH 5.5 and 97% at pH 7.4, but decreased significantly outside this pH range. At 50 °C, maximum retention of active protein was at pH 5.5, with 67% active protein remaining after 4 weeks. At all other pH values, retention of activity was significantly lower, in particular at pH 3.0, 5.5 and 11 only  $\leq 10\%$  active protein remained. A similar stability profile was observed for another  $V_{NAR}$  (clone 27P-1) in short-term (1 day) trials at pHs 3, 7.4 and 9 at 37 and 60 °C (data not shown).

**Figure 1.** Retention of active variable new antigen receptor Variable New Antigen Receptor ( $V_{NAR}$ ) 4A-1 protein following heating at various pHs and temperatures (a) for 1 day and (b) for 4 weeks.

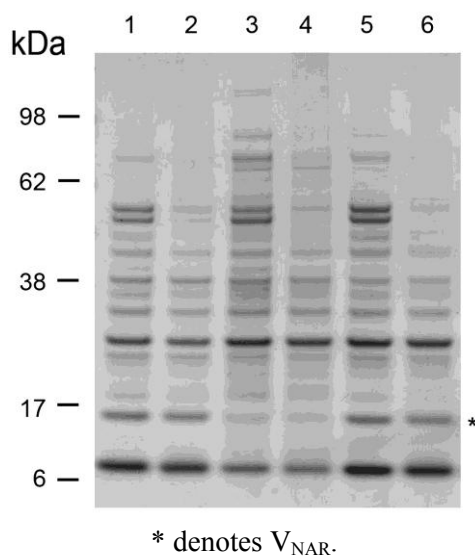


## 2.2. Thermostability of $V_{NARS}$ and Mabs in Liquid and Lyophilized Formats

Given the very good stability of this model  $V_{NAR}$ , we decided to further examine a family of  $V_{NARS}$  (12Y-2, 14M-15 and 14I1M-15) which target AMA-1 from *Plasmodium falciparum* (strain 3D7) using a variety of stability assays.  $V_{NARS}$  14M-15 and 14I1M-15 are affinity matured variants of 12Y-2, and have binding affinities of 31, 5 and 708 nM, respectively for AMA-1 [8].

In the first instance,  $V_{NARS}$  which had been semi-purified as periplasmic extracts were heated to 100 °C for 15 min. Using SDS-PAGE, soluble protein content was then compared between untreated and heat treated samples (Figure 2). It was apparent that whilst a reasonable proportion of host cell proteins were heat labile, the  $V_{NARS}$  were unaffected by the heat treatment.

**Figure 2.** SDS-PAGE analysis of  $V_{NARS}$  in *Escherichia coli* periplasmic extracts before and after heat treatment at 100 °C for 15 min. **Lane 1:** untreated 12Y-2, **Lane 2:** heat treated 12Y-2, **Lane 3:** untreated 14M-15, **Lane 4:** heat treated 14M-15, **Lane 5:** untreated 14I1M-15, **Lane 6:** heat treated 14I1M-15.



Given these promising results, purified  $V_{NARS}$  12Y-2 and 14I1M-15 were then compared to two mAbs 5G8 and 1F9 at 45 °C in liquid format in short term (0–72 h) and long term (1–4 weeks) stability trials (Figure 3a), and in lyophilized format in long term trials only (Figure 3b). The mAbs 5G8 and 1F9 likewise target AMA-1 [10]. The affinity of 5G8 for AMA-1 is 175 nM [9] and the affinity of 1F9 for AMA-1 is 950 pM (Appendix Figure A2).

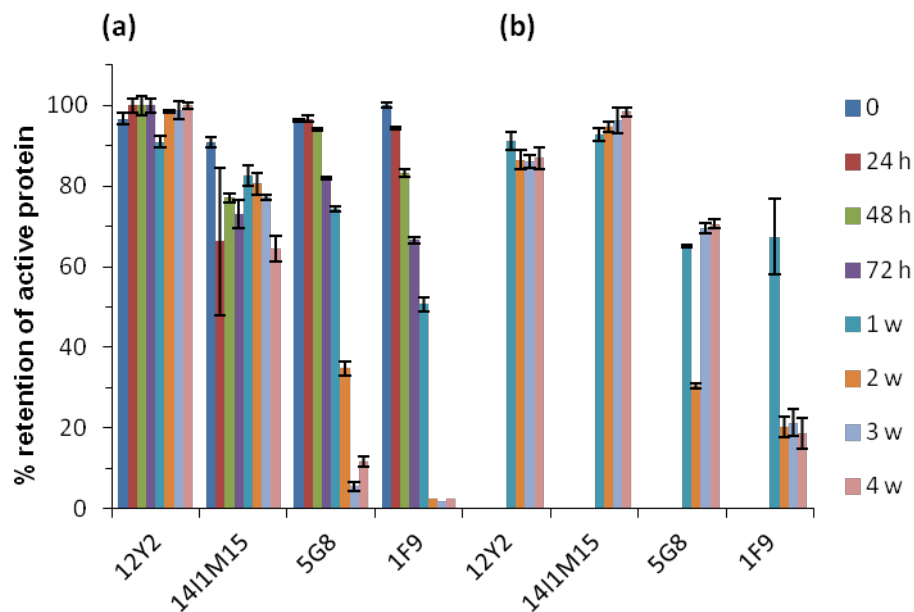
The concentration of active protein ( $V_{NAR}$  or mAb) remaining after each treatment was evaluated using SPR biosensor (Biacore T200) analyses. This method relied upon determination of residual binding activity to AMA-1 protein of treated samples by comparing their binding responses to those obtained with the starting untreated sample. By extrapolating against a calibration curve, generated using the starting material, the residual active concentration of treated samples was determined.

In short term trials in liquid at 45 °C,  $V_{NAR}$  12Y-2 retained 100% activity after 72 h, whereas 14I1M-15 retained 73% activity. By comparison, under the same conditions, mAbs 5G8 and 1F9 retained 82% and 67% activity, respectively. Additional analyses showed that after 72 h at 60 °C, the only binder to retain activity was 12Y-2, with 20% activity remaining (Appendix Figure A3).

In long term trials  $V_{NARS}$  were generally more stable and performed consistently well in both formats, by comparison with mAbs (Figure 3). In liquid format after heating at 45 °C for 4 weeks, 100 and 65% activity was retained by 12Y-2 and 14I1M-15, respectively. By comparison, 12 and 2% activity was retained by 5G8 and 1F9, respectively, under these conditions. Heating at 60 °C abolished most of the activity of all antibodies in liquid format after 1 week (Appendix Figure A3).

Retention of activity of lyophilized  $V_{NARS}$  was excellent (Figure 3b). Greater than 86% activity was retained by 12Y-2 and 14I1M-15, regardless of temperature or incubation period. For incubation periods longer than 72 h, both mAbs performed better in lyophilized format rather than in liquid format. The 5G8 and 1F9 retained 71% and 19% activity, respectively, after 4 weeks at 45 °C.

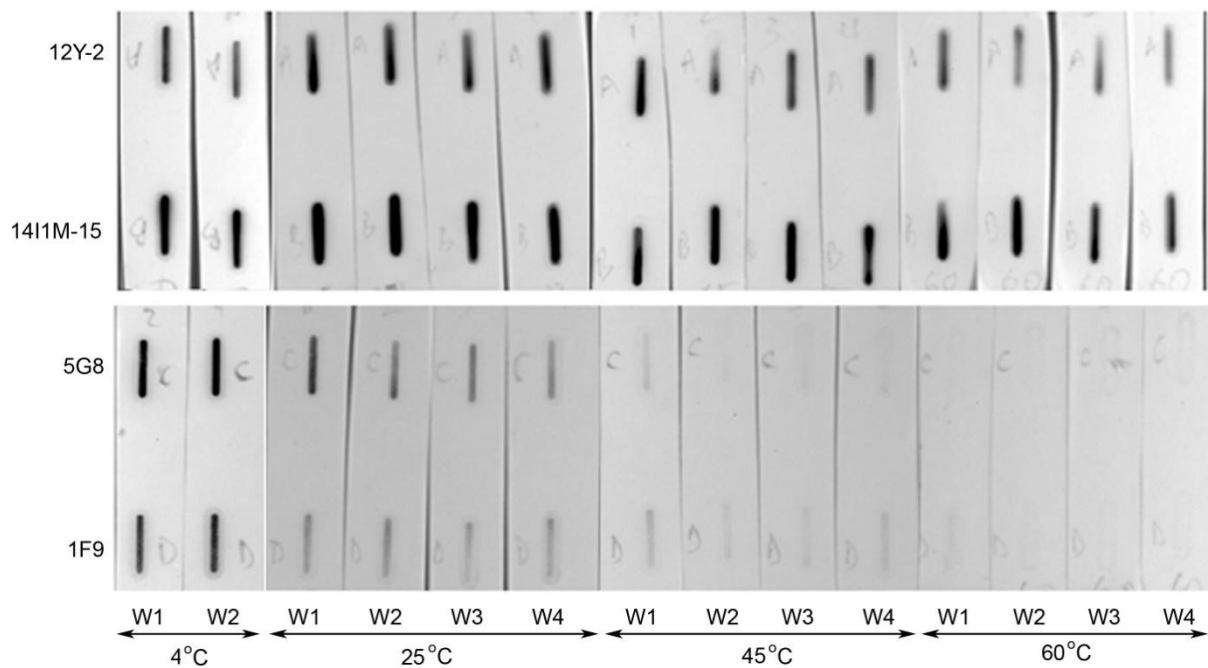
**Figure 3.** Retention of active  $V_{NARS}$  12Y-2 and 14I1M-15, and monoclonal antibodies (mAbs) 5G8 and 1F9 following heating at 45 °C in (a) liquid and (b) lyophilized formats, as determined by biosensor analysis. The standard deviation for 1F9 time points 2, 3 and 4 weeks was  $\leq 30\%$ , error bars are shown for all other values.



Next, we extended these results to include  $V_{NARS}$  and mAbs immobilized on nitrocellulose strips that had been incubated at 25, 45 and 60 °C for 4 weeks (Figure 4). To determine retention of activity the heat-treated immobilized antigens were probed with the cognate malarial protein, AMA-1. After incubation for 4 weeks, both  $V_{NARS}$  retained almost complete activity at all temperatures, evidenced by excellent binding to AMA-1 protein. By comparison, both mAbs lost significant activity after heating at 45 °C for 4 weeks, and no activity was detectable after heating at 60 °C for 4 weeks.

Most of the current rapid diagnostic tests (RDTs) for malaria are based on antigen detection by monoclonal antibodies immobilized onto nitrocellulose membranes. Although in use for more than 10 years, issues about their thermostability have affected confidence with their performance [11–13]. Our results are clear evidence of how the activity of mAbs onto nitrocellulose membranes can be impaired by temperatures commonly found in endemic areas ( $>40$  °C), and that  $V_{NARS}$  are an attractive option for the improvement of RDTs for malaria.

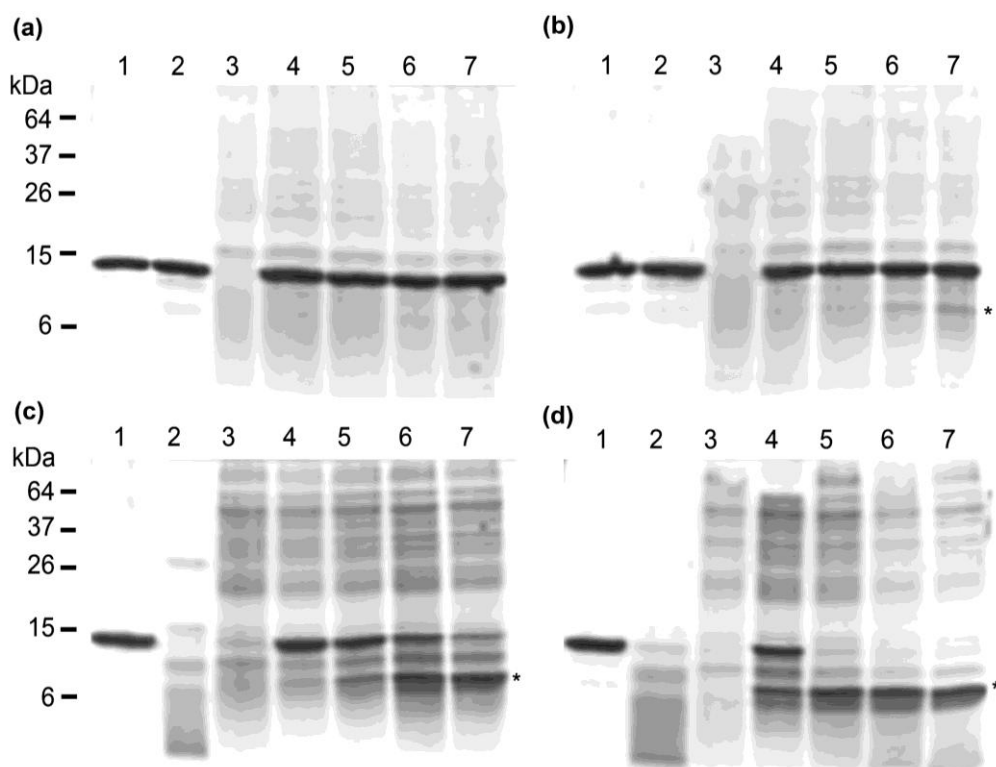
**Figure 4.** Retention of activity of  $V_{NARS}$  and monoclonal antibodies immobilized on nitrocellulose, following heating at various temperatures and time periods (W = week).



### 2.3. Thermostability of $V_{NARS}$ in Biological Samples

To further extend these results to possible *in vitro* applications involving contact with biological samples, or for possible future *in vivo* administration for gut-specific infectious diseases or cancers, the  $V_{NAR}$  antibody fragment 14M-15 was exposed to murine stomach scrapings (acidic, pH 5) and intestinal samples (a protease-rich environment). After 1 hour exposure to stomach scrapings at 4 °C, there was no evidence of  $V_{NAR}$  degradation whereas at 37 °C there was a small amount of degradation evidenced by the release of a ~12 kDa fragment (Figure 5). In the control sample incubated at pH 3, 14M-15 remained intact. Incubation in the presence of intestinal scrapings resulted in time- and temperature dependent partial-degradation of 14M-15 to a ~11 kDa fragment. At 4 °C, degradation was initiated at  $\leq 10$  min and intensified with incubation time. After 60 min approximately 75% of 14M-15 was degraded. Degradation at 37 °C was initiated immediately (at  $\leq 1$  min) and by 30 min was complete, with a single 11 kDa fragment of 14M-15 remaining. An additional  $V_{NAR}$ , Help6, which binds Hepatitis B precore protein responded in exactly the same manner to incubation in these murine samples (data not shown). N-terminal sequencing of the  $V_{NAR}$  fragment confirmed the N-terminus was intact, thus cleavage occurred approximately 3 kDa from the C-terminus of 14M-15 which is in a conserved framework region at the framework CDR3 junction. Given the framework sequence is largely conserved, this same stability response to gastrointestinal proteases would likely be universal among our  $V_{NAR}$  clones.

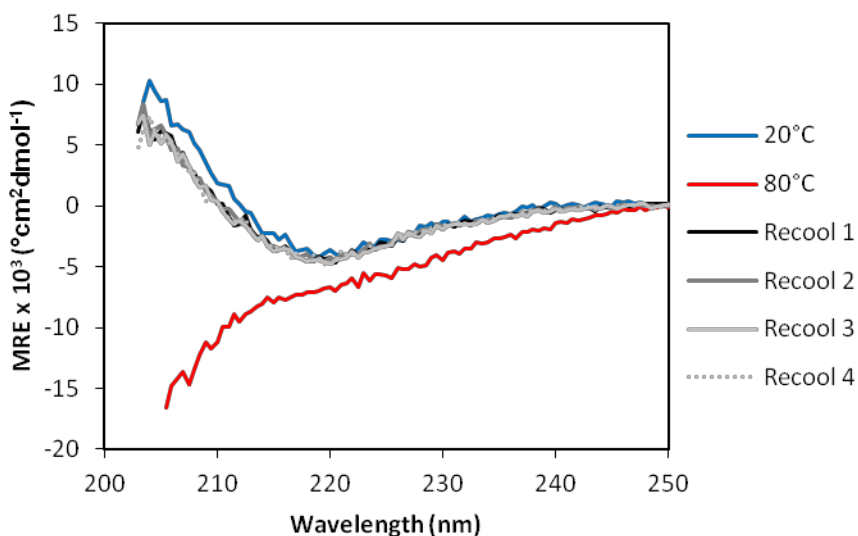
**Figure 5.** SDS-PAGE analysis of  $V_{NARS}$  during incubation with murine stomach and intestinal scrapings. **(a)** Incubation at 4 °C, **Lane 1:** untreated 14M-15, **Lane 2:** 14M-15 with pH 3 glycine, **Lane 3:** Murine stomach sample, **Lane 4:** Murine stomach sample with 14M-15, 1 min incubation, **Lane 5:** Murine stomach sample with 14M-15, 10 min incubation, **Lane 6:** Murine stomach sample with 14M-15, 30 min incubation, **Lane 7:** Murine stomach sample with 14M-15, 60 min incubation. **(b)** Incubation at 37 °C, loading same as **(a)**. **(c)** Incubation at 4 °C, **Lane 1:** untreated 14M-15, **Lane 2:** 14M-15 with proteinase K, **Lane 3:** Murine intestinal sample, **Lane 4:** Murine intestinal sample with 14M-15, 1 min incubation, **Lane 5:** Murine intestinal sample with 14M-15, 10 min incubation, **Lane 6:** Murine intestinal sample with 14M-15, 30 min incubation, **Lane 7:** Murine intestinal sample with 14M-15, 60 min incubation. **(d)** Incubation at 37 °C, loading same as **(c)**. \*14M-15 degradation products resulting from acid or protease activity.



#### 2.4. Analysis of Secondary Structure by Circular Dichroism Spectroscopy

In order to investigate the secondary structure and thermal stability of the  $V_{NAR}$  12Y-2 scaffold, we conducted circular dichroism (CD) spectroscopy at low and high temperatures. At 20 °C the secondary structure of the  $V_{NAR}$  was predominantly  $\beta$ -strand as evidenced by an absorbance minimum at 218 nm and maximum at 195 nm [14] (Figure 6, blue trace). When heated to 80 °C, a significant decrease in the ellipticity at 205 nm was observed, indicating that 12Y-2 adopts a predominantly random coil structure at the high temperature consistent with unfolding of the scaffold (Figure 6, red trace). However, upon re-cooling to 20 °C (Figure 6, black trace) the CD spectrum adopted a similar profile to that obtained prior to heating. Repeated heating-cooling cycles resulted in reproducible results (Figure 6, gray traces), suggesting the protein is very stable at high temperatures due to an ability to refold reversibly upon thermal denaturation.

**Figure 6.** Secondary structure and thermostability of 12Y-2 measured by circular dichroism (CD) spectroscopy. Wavelength scans of 12Y-2 were taken at 20 °C and 80 °C, and repeated four times following cycles of heating to 80 °C and cooling to 20 °C (Recool 1–4).



Immunoglobulin new antigen receptors (IgNARs) have evolved to function in antigen recognition via single variable domains ( $V_{\text{NARS}}$ ). Single Ig binding domains engineered from paired VH-VL origins typically show a high degree of aggregation due to exposure of hydrophobic faces to solvent, although emerging methods may overcome this tendency [15]. Immunoglobulin domains are inherently stable by virtue of their secondary and tertiary structures. The arrangement of antiparallel  $\beta$ -strands is optimized for H-bond formation and van der Waals interactions between the strands to form two  $\beta$ -sheets. The size and tertiary structure of shark  $V_{\text{NARS}}$  parallel nanobodies engineered from camelid VHs, which akin to IgNARs comprise paired heavy chains and no associated light chains [16]. As such, nanobodies and  $V_{\text{NARS}}$  share comparable physicochemical properties including high thermal stability and nM–pM antigen binding affinities [17]. The finding that by CD analysis the  $V_{\text{NAR}}$  scaffold refolds following repeated heating-cooling cycles (Figure 6), suggests that the loss of activity observed in liquid formats for prolonged periods and at extreme pH (Figures 1 and 3) is due to irreversible damage to the scaffold such as reduction of the framework disulfide bond or loss of local structure which effects CDR3 conformation.

Particular applications of biologic diagnostic reagents include (i) disease detection and discrimination in hand held point of care devices (with major demand in developing countries or regions or where refrigeration is unreliable or unavailable [18]); (ii) molecular *in vivo* imaging [19] and (iii) drug or radionuclide delivery via antibody drug conjugates [20]. The stability of several  $V_{\text{NARS}}$  at elevated temperatures in liquid, lyophilized and immobilized formats suggests this scaffold has excellent suitability for diagnostic markets. Our findings demonstrate that it would be feasible to customize storage parameters for individual diagnostic  $V_{\text{NARS}}$ , given that 100% activity of  $V_{\text{NAR}}$  4A-1 was retained at pH 5.5 and 37 °C (Figure 1). Furthermore, large-scale production of  $V_{\text{NARS}}$  could be expedited using heating and subsequent cooling as a simple and inexpensive purification step as has been explored for recombinant camelid antibodies [21], and as we have shown in preliminary studies (Figure 2).

Beyond protein engineering for affinity, there exists the possibility of modification to enhance  $V_{\text{NAR}}$  pharmacokinetic (PK) properties such as stability and half-life. For *in vivo* applications the target tissue and mode of delivery will dictate specific traits required of potential  $V_{\text{NAR}}$  candidates. One approach to improve PK properties was recently reported by Müller *et al.* [22] whereby two- and three-domain  $V_{\text{NAR}}$  constructs showed increased half-life in mouse, rat and monkey models. It is conceivable that residues that are particularly important for stability may be pinpointed and appropriately modified, in much the same manner that affinity-enhancing and hallmark mutations have been comprehensively mapped for  $V_{\text{NAR}}$  domains in the study of Fennel *et al.* [23]. Our analysis of  $V_{\text{NAR}}$  stability in pH and temperature extremes provides a ready model system for such experimentation.

### 3. Experimental Section

#### 3.1. Nucleic Acid Isolation and Cloning

$V_{\text{NAR}}$  4A-1 was isolated from a  $V_{\text{NAR}}$  phagemid library in which a 6-residue CDR1 region was fully randomized and a CDR3 region varied in length from 10–20 residues and was fully randomized (“ $V_{\text{NAR}}$  10-20 library”). The  $V_{\text{NAR}}$  10–20 library was constructed and biopanned as described elsewhere [5,24] with the following exceptions: mAb 5G8 was coated onto Maxisorb Immuno-plates (Nunc, Germany) at a concentration of 10  $\mu\text{g}/\text{mL}$ , plates were rinsed with phosphate buffered saline (PBS, 137 mM NaCl, 2.7 mM KCl, 10 mM  $\text{Na}_2\text{HPO}_4$ , 2 mM  $\text{KH}_2\text{PO}_4$ , pH 7.4) then blocked with PBS/5% (w/v) skim milk powder (Diploma, Australia) for 3 h at room temperature (RT) and then incubated with freshly prepared phage particles in PBS/0.5% (w/v) skim milk powder for 1 h at RT, after incubation plates were washed (round 1: 2  $\times$  PBS; round 2: 4  $\times$  PBS/0.1% Tween20, 2  $\times$  PBS; round 3: 6  $\times$  PBS/0.1% (v/v) Tween20, 2  $\times$  PBS) then phage were eluted using 0.1 M glycine, pH 2.2 and neutralized with 1.5 M Tris-HCl, pH 8.0. Construction of  $V_{\text{NAR}}$  error prone PCR mutagenised libraries, panning against AMA-1 (type 3D7) [25] and isolation of clones 12Y-2, 14M-15 and 14I1M-15 have been described previously [5,8,24].

$V_{\text{NARS}}$  4A-1, 12Y-2, 14M-15 and 14I1M-15 were expressed from pGC [26] using the cell line *E. coli* TG1 [*supE thi-1  $\Delta$ (lac-proAB)  $\Delta$ (mcrB-hsdSM)5* ( $r_K^- m_K^-$ ) (*F' traD36 proAB lacI<sup>q</sup>Z $\Delta$ M15*)] (Stratagene, USA). *E. coli* transformants were maintained in 2YT medium supplemented with 100  $\mu\text{g}/\text{mL}$  ampicillin and 2.0% (w/v) glucose. Solid medium contained 2.0% (w/v) Bacto-agar. Transformation of *E. coli* was by standard procedures using electro-competent cells. DNA clones were sequenced on both strands using a BigDye terminator cycle sequencing kit (Applied Biosystems, Foster City, CA., USA) and analyzed on an a 3730  $\times$  1 96-capillary automated DNA Sequencer (Applied Biosystems, Foster City, CA., USA).

#### 3.2. Soluble Expression of $V_{\text{NAR}}$ Constructs from Expression Vector pGC

Recombinant proteins were expressed in the bacterial periplasm as described previously [27,28]. Proteins were purified from the periplasm by the method of Minsky [29] and used either as crude fractions or purified further by affinity chromatography using ANTI-FLAG M2 Affinity gel resin (2–10  $\times$  1 cm) (Sigma, St. Louis, MO, USA). Protein elution was with 0.1 M glycine (pH 3) or ImmunoPure<sup>TM</sup> gentle elution buffer (Pierce, USA). Neutralized proteins were dialyzed extensively

against PBS, pH 7.4, and then concentrated over a YM-3 (3 kDa cut-off) membrane (Amicon, Japan). Apical membrane antigen 1 (AMA-1) from *Plasmodium falciparum* strain 3D7 was expressed recombinantly and purified as previously described [30].

### 3.3. Thermal and pH Stability of $V_{NARS}$ and mAbs

#### 3.3.1. pH Stability of $V_{NAR}$ 4A-1

Separate 50  $\mu$ L aliquots of purified recombinant  $V_{NAR}$  4A-1 (specific for mAb 5G8) at 0.12 mg/mL were adjusted to pHs 3, 5.5 (using 0.2 M  $\text{Na}_2\text{HPO}_4$  and 0.1 M citric acid), pH 7.4 (using PBS), and pHs 8.5, 11.0 (using 25 mM borax buffer) then incubated at 4, 37 and 50 °C for 24 h and 1, 2, 3, 4 weeks. Unheated control samples were stored at -20 °C throughout. Following incubation, samples were neutralized with 1 M Tris at pH 11.5 (for samples at pH 3.0 and 5.5) or with 1 M HCl (for samples at pH 8.5 and 11.0).

#### 3.3.2. Heating $V_{NARS}$ in Periplasmic Extracts at 100 °C

Separate 100  $\mu$ L aliquots of  $V_{NARS}$  12Y-2, 14M-15, 14I1M-15 and 22A-2 in periplasmic extracts were incubated at RT or 100 °C for 15 min then clarified by centrifugation for 5 min. The resulting soluble proteins were analyzed by SDS-PAGE.

#### 3.3.3. Heating $V_{NARS}$ and mAbs at 45 °C and 60 °C for up to 4 Weeks

Separate 40  $\mu$ L aliquots of purified recombinant  $V_{NARS}$  (12Y-2, 14I1M-15) and monoclonal antibodies (1F9, 5G8, Monoclonal Antibody Facility, Walter & Eliza Hall Institute Biotechnology Centre, Melbourne, Australia) all at 1 mg/mL were incubated in liquid and lyophilized formats at 45 °C and 60 °C, for 24, 48 and 72 h and 1, 2, 3 and 4 weeks and then stored at 4 °C until analysis. Unheated control samples were stored at 4 °C throughout.

### 3.4. Biosensor Analysis of $V_{NAR}$ Proteins

All Surface Plasmon Resonance (SPR) biosensor analyses were performed at 25 °C using Biacore 1000, Biacore T100 (GE Healthcare, Uppsala, Sweden), SensiQ Pioneer (SensiQ Technologies, Oklahoma City, OK) and ProteOn XPR36 (Bio-Rad, Hercules, CA) platforms with instrumental fluidics primed in 1  $\times$  HBS-EP + [10 mM HEPES, 150 mM NaCl, 3 mM EDTA 0.05% (v/v) surfactant P20, pH 7.4].

#### 3.4.1. Immobilization of Recombinant Proteins

Coupling of AMA-1 on CM5 sensor chips (Biacore) was achieved essentially as described previously [5]. Briefly, the chip surface was activated with a 7 min injection of a freshly prepared 1:1 mixture of 50 mM NHS : 200 mM EDC. Protein coupling was achieved by a single 7 min injection solution (23  $\mu$ g/mL in 10 mM sodium acetate, pH 4.0). To deactivate residual reactive sites, AMA-1 coupling was followed by a 7 min injection of 1 M ethanolamine (pH 8.5). Immobilization of AMA-1 protein on the surface of a GLM chip (ProteOn) was achieved in a similar manner with the following

differences: (1) chip activation 50:50 mixture consisted of a sulfo-NHS at 5 mM and EDC at 20 mM and (2) injections of activation mixture, ligand solution and deactivation solution were all performed at 30  $\mu\text{L}/\text{min}$  for 5 min. Both coupling procedures typically resulted in  $>8,000$  Response Units (1 RU; 1000 RU = 1 ng of protein/ $\text{mm}^2$ ) of AMA-1 protein being coupled to either of the two chips. Coupling of 5G8 IgG (target antigen for 4A-1 IgNAR) on a GLM chip was performed using a similar method to that described above for AMA-1 except that the 5G8 IgG protein solution was diluted to 20  $\mu\text{g}/\text{mL}$  in 10 mM sodium acetate, pH 4.5. Approximately 7,600 RU of IgG protein was coupled to the chip surface.

### 3.4.2. Active Concentration Determinations

Fully automated SPR-based concentration assay [31] was utilized for the determination of the residual AMA-1 binding activity in diversely treated  $V_{\text{NAR}}$  and IgG antibody samples. The method was configured as a direct detection assay with quantification against a calibration standard, that being an untreated sample stored at 4  $^{\circ}\text{C}$  ( $t = 0$ ). In case of Biacore T100 assay, a standard curve was established by serially injecting ' $t = 0$ ' calibration samples at 0, 250, 500, 1,000, 2,000, 4,000, 8,000 and 1,600 ng/mL over the AMA-1 immobilized sensor chip. Assay conditions were: flow rate, 10  $\mu\text{L}/\text{min}$ , contact time, 1 min; regeneration: 100  $\mu\text{L}/\text{min}$  for 10 s of 10 mM glycine pH 2.2. Binding responses, taken 10 s after sample injection was stopped, were plotted against the injected concentration. Residual active concentrations of heated samples were quantified by interpolation of binding responses against the standard curve. A similar approach was adopted for the ProteOn XPR36. Standard curve was established by a parallel injection of six different ' $t = 0$ ' sample concentrations (500, 1,000, 2,000, 4,000, 8,000 ng/mL) across the immobilized AMA-1 or 5G8 IgG protein at 25  $\mu\text{L}/\text{min}$  for 60 s. Residual active concentrations of unknown samples were determined by injecting six samples simultaneously and comparing their initial binding rates (at  $t = 5\text{--}20$  s) to those generated by the calibration standards. Bound samples were regenerated from the surface with a single injection of 10 mM glycine pH 2.2 at 100  $\mu\text{L}/\text{min}$  for 15 s.

### 3.5. Nitrocellulose Dot Blot and Western Analysis

Varying amounts of  $V_{\text{NARS}}$  (1  $\mu\text{g}$  of 12Y-2, 0.32  $\mu\text{g}$  of 14I1M-15) and mAbs (0.05  $\mu\text{g}$  of 5G8, 0.01  $\mu\text{g}$  of 1F9) were dot blotted onto nitrocellulose membrane (Osmonics, Minnetonka, MN, USA) in 100  $\mu\text{L}$  PBS using a slot blot manifold. These amounts were pre-determined in earlier titration experiments to provide equivalent signal intensity (data not shown). Twenty two strips of nitrocellulose containing each protein were incubated at 4, 25, 45 and 60  $^{\circ}\text{C}$ . Strips were removed weekly from all incubation temperatures and stored at 4  $^{\circ}\text{C}$  until testing. The nitrocellulose strips were cut into two, separating  $V_{\text{NARS}}$  from mAbs and blocked in 10% (w/v) skim milk powder for 1 h. Between each step the membranes were washed 3 times with PBS containing 0.1% (v/v) Tween20. Antibodies were diluted in PBS containing 0.1% (v/v) Tween20. AMA-1 was added at 5  $\mu\text{g}/\text{mL}$  in 5% (w/v) milk powder and incubated for 2 h at room temperature. Rabbit anti-AMA-1 serum was then added at 1:3,000 dilution and incubated for 1 h. Anti-rabbit-HRP (GE Healthcare, WI, USA) was added at 1:1,000 dilution and incubated for 1 h then signal was developed using SuperSignal West Pico Chemiluminescent Signal (ThermoScientific, Rockford, IL, USA).

### 3.6. Exposure of $V_{\text{NAR}}$ 14M-15 to Murine stomach and Intestinal Scrapings

Gastric and intestinal samples were obtained from mice (P. Sutton, School of Veterinary Science, University of Melbourne, Australia) as described previously [32,33]. The samples were homogenised and sonicated in PBS containing 1% (v/v) Triton X 100 and then the total protein concentration was determined via BCA assay (BioRad, Hercules, CA, USA). Aliquots of  $V_{\text{NAR}}$  14M-15 (15  $\mu\text{g}$ ) were incubated with stomach or intestinal samples (33  $\mu\text{g}$ ), unbuffered, in a total volume of 45  $\mu\text{L}$  for 1, 10, 30 or 60 min at 0 and 37 °C. Negative controls were water, glycine (pH 3) or protease K in place of stomach and intestinal samples. Following incubation, samples were analyzed by SDS-PAGE and Western blotting in order to visualize VNAR fragmentation or degradation.

### 3.7. Circular Dichroism Spectroscopy

CD spectra were recorded using an AVIV Model 420 CD spectrometer using similar methods to those described previously [34]. Wavelength scans were performed using a 1 mm quartz cuvette at 20 °C and 80 °C from 190 and 250 nm. Proteins were solubilized in PBS at a concentration of 0.15 mg/mL. Spectra were baseline-corrected by subtracting corresponding buffer scans collected under identical conditions.

## 4. Conclusions

Single domain shark  $V_{\text{NARS}}$  can be readily selected against antigens of diagnostic value. When expressed recombinantly they show excellent stability at elevated temperatures over prolonged periods in liquid, lyophilized and immobilized formats, particularly in comparison with mAbs. Furthermore, the  $V_{\text{NAR}}$  domains show very good stability properties at pH extremes, with resistance to proteolytic cleavage. Together these data demonstrate the versatility of these unique single domains and their amenability to more complex and varied diagnostic applications.

## Acknowledgments

This work was supported by the National Health and Medical Research Council of Australia (ID 487339), a grant from the National Institutes of Health (NIH RO1AI59229) and through funding from The Foundation for Innovative New Diagnostics (FIND). Matthew A. Perugini acknowledges the Australian Research Council for Future Fellowship support (FT0991245). The authors thank Robin Anders for provision of recombinant AMA-1, Denison Chang and Meghan Hattarki for technical assistance and Phil Sutton for supplying the murine stomach and intestine samples. Michael Foley declares a competing financial interest.

## References and Notes

1. Murray, C.K.; Gasser, R.A., Jr.; Magill, A.J.; Miller, R.S. Update on rapid diagnostic testing for malaria. *Clin. Microbiol. Rev.* **2008**, *21*, 97–110.

2. Roux, K.H.; Greenberg, A.S.; Greene, L.; Strelets, L.; Avila, D.; McKinney, E.C.; Flajnik, M.F. Structural analysis of the nurse shark (new) antigen receptor (nar): Molecular convergence of nar and unusual mammalian immunoglobulins. *Proc. Natl. Acad. Sci. USA* **1998**, *95*, 11804–11809.
3. Streltsov, V.A.; Varghese, J.N.; Carmichael, J.A.; Irving, R.A.; Hudson, P.J.; Nuttall, S.D. Structural evidence for evolution of shark ig new antigen receptor variable domain antibodies from a cell-surface receptor. *Proc. Natl. Acad. Sci. USA* **2004**, *101*, 12444–12449.
4. Stanfield, R.L.; Dooley, H.; Flajnik, M.F.; Wilson, I.A. Crystal structure of a shark single-domain antibody V region in complex with lysozyme. *Science* **2004**, *305*, 1770–1773.
5. Nuttall, S.D.; Humberstone, K.S.; Krishnan, U.V.; Carmichael, J.A.; Doughty, L.; Hattarki, M.; Coley, A.M.; Casey, J.L.; Anders, R.F.; Foley, M.; *et al.* Selection and affinity maturation of IgNAR variable domains targeting *Plasmodium falciparum* AMA-1. *Proteins* **2004**, *55*, 187–197.
6. Kopsidas, G.; Roberts, A.S.; Coia, G.; Streltsov, V.A.; Nuttall, S.D. *In vitro* improvement of a shark IgNAR antibody by Q $\beta$  replicase mutation and ribosome display mimics *in vivo* affinity maturation. *Immunol. Lett.* **2006**, *107*, 163–168.
7. Simmons, D.P.; Abregu, F.A.; Krishnan, U.V.; Proll, D.F.; Streltsov, V.A.; Doughty, L.; Hattarki, M.K.; Nuttall, S.D. Dimerisation strategies for shark IgNAR single domain antibody fragments. *J. Immunol. Methods* **2006**, *315*, 171–184.
8. Henderson, K.A.; Streltsov, V.A.; Coley, A.M.; Dolezal, O.; Hudson, P.J.; Batchelor, A.H.; Gupta, A.; Bai, T.; Murphy, V.J.; Anders, R.F.; *et al.*, Structure of an IgNAR-AMA1 complex: Targeting a conserved hydrophobic cleft broadens malarial strain recognition. *Structure* **2007**, *15*, 1452–1466.
9. Simmons, D.P.; Streltsov, V.A.; Dolezal, O.; Hudson, P.J.; Coley, A.M.; Foley, M.; Proll, D.F.; Nuttall, S.D. Shark IgNAR antibody mimotopes target a murine immunoglobulin through extended CDR3 loop structures. *Proteins* **2008**, *71*, 119–130.
10. Coley, A.M.; Campanale, N.V.; Casey, J.L.; Hodder, A.N.; Crewther, P.E.; Anders, R.F.; Tilley, L.M.; Foley, M. Rapid and precise epitope mapping of monoclonal antibodies against *Plasmodium falciparum* AMA-1 by combined phage display of fragments and random peptides. *Protein Eng.* **2001**, *14*, 691–698.
11. Bell, D.; Wongsrichanalai, C.; Barnwell, J.W. Ensuring quality and access for malaria diagnosis: How can it be achieved? *Nat. Rev. Microbiol.* **2006**, *4*, S7-20.
12. Chiodini, P.L.; Bowers, K.; Jorgensen, P.; Barnwell, J.W.; Grady, K.K.; Luchavez, J.; Moody, A.H.; Cenizal, A.; Bell, D. The heat stability of *Plasmodium* lactate dehydrogenase-based and histidine-rich protein 2-based malaria rapid diagnostic tests. *Trans. R. Soc. Trop. Med. Hyg.* **2007**, *101*, 331–337.
13. Ashley, E.A.; Touabi, M.; Ahrer, M.; Hutagalung, R.; Htun, K.; Luchavez, J.; Dureza, C.; Proux, S.; Leimanis, M.; Lwin, M.M., *et al.* Evaluation of three parasite lactate dehydrogenase-based rapid diagnostic tests for the diagnosis of *falciparum* and *vivax* malaria. *Malar. J.* **2009**, *8*, 241.
14. Greenfield, N.J. Using circular dichroism spectra to estimate protein secondary structure. *Nat. Protoc.* **2006**, *1*, 2876–2890.
15. Dudgeon, K.; Rouet, R.; Kokmeijer, I.; Schofield, P.; Stolp, J.; Langley, D.; Stock, D.; Christ, D. General strategy for the generation of human antibody variable domains with increased aggregation resistance. *Proc. Natl. Acad. Sci. USA* **2012**, *109*, 10879–10884.

16. Hamers-Casterman, C.; Atarhouch, T.; Muyldermans, S.; Robinson, G.; Hamers, C.; Songa, E.B.; Bendahman, N.; Hamers, R. Naturally occurring antibodies devoid of light chains. *Nature* **1993**, *363*, 446–448.
17. Hussack, G.; Arbabi-Ghahroudi, M.; van Faassen, H.; Songer, J.G.; Ng, K.K.; MacKenzie, R.; Tanha, J. Neutralization of *Clostridium difficile* toxin a with single-domain antibodies targeting the cell receptor binding domain. *J. Biol. Chem.* **2011**, *286*, 8961–8976.
18. Urdea, M.; Penny, L.A.; Olmsted, S.S.; Giovanni, M.Y.; Kaspar, P.; Shepherd, A.; Wilson, P.; Dahl, C.A.; Buchsbaum, S.; Moeller, G.; *et al.* Requirements for high impact diagnostics in the developing world. *Nature* **2006**, *444*, 73–79.
19. Romer, T.; Leonhardt, H.; Rothbauer, U. Engineering antibodies and proteins for molecular *in vivo* imaging. *Curr. Opin. Biotechnol.* **2011**, *22*, 882–887.
20. Adair, J.R.; Howard, P.W.; Hartley, J.A.; Williams, D.G.; Chester, K.A. Antibody-drug conjugates—A perfect synergy. *Expert Opin. Biol. Ther.* **2012**, *12*, 1191–1206.
21. Olichon, A.; Schweizer, D.; Muyldermans, S.; de Marco, A. Heating as a rapid purification method for recovering correctly-folded thermotolerant VH and VHH domains. *BMC Biotechnol.* **2007**, *7*, 7.
22. Muller, R.M.; Saunders, K.; Grace, C.; Jin, M.; Piche-Nicholas, N.; Steven, J.; O'Dwyer, R.; Wu, L.; Khetemene, L.; Vugmeyster, Y.; *et al.* Improving the pharmacokinetic properties of biologics by fusion to an anti-HSA shark VNAR domain. *mAbs* **2012**, *4*, 673–685.
23. Fennell, B.J.; Darmanin-Sheehan, A.; Hufton, S.E.; Calabro, V.; Wu, L.; Muller, M.R.; Cao, W.; Gill, D.; Cunningham, O.; Finlay, W.J. Dissection of the IgNAR V domain: Molecular scanning and orthologue database mining define novel ignar hallmarks and affinity maturation mechanisms. *J. Mol. Biol.* **2010**, *400*, 155–170.
24. Nuttall, S.D.; Krishnan, U.V.; Doughty, L.; Pearson, K.; Ryan, M.T.; Hoogenraad, N.J.; Hattarki, M.; Carmichael, J.A.; Irving, R.A.; Hudson, P.J. Isolation and characterization of an IgNAR variable domain specific for the human mitochondrial translocase receptor tom70. *Eur. J. Biochem.* **2003**, *270*, 3543–3554.
25. Hodder, A.N.; Crewther, P.E.; Anders, R.F. Specificity of the protective antibody response to apical membrane antigen 1. *Infect. Immun.* **2001**, *69*, 3286–3294.
26. Coia, G.; Ayres, A.; Lilley, G.G.; Hudson, P.J.; Irving, R.A. Use of mutator cells as a means for increasing production levels of a recombinant antibody directed against Hepatitis B. *Gene* **1997**, *201*, 203–209.
27. Nuttall, S.D.; Krishnan, U.V.; Doughty, L.; Nathanielsz, A.; Ally, N.; Pike, R.N.; Hudson, P.J.; Kortt, A.A.; Irving, R.A. A naturally occurring NAR variable domain binds the Kgp protease from *Porphyromonas gingivalis*. *FEBS Lett.* **2002**, *516*, 80–86.
28. Nuttall, S.D.; Rousch, M.J.; Irving, R.A.; Hufton, S.E.; Hoogenboom, H.R.; Hudson, P.J. Design and expression of soluble CTLA-4 variable domain as a scaffold for the display of functional polypeptides. *Proteins* **1999**, *36*, 217–227.
29. Minsky, A.; Summers, R.G.; Knowles, J.R. Secretion of beta-lactamase into the periplasm of *Escherichia coli*: Evidence for a distinct release step associated with a conformational change. *Proc. Natl. Acad. Sci. USA* **1986**, *83*, 4180–4184.

30. Gupta, A.; Bai, T.; Murphy, V.; Strike, P.; Anders, R.F.; Batchelor, A.H. Refolding, purification, and crystallization of apical membrane antigen 1 from *Plasmodium falciparum*. *Protein Expr. Purif.* **2005**, *41*, 186–198.
31. Gapper, L.W.; Copestake, D.E.; Otter, D.E.; Indyk, H.E. Analysis of bovine immunoglobulin g in milk, colostrum and dietary supplements: A review. *Anal. Bioanal. Chem.* **2007**, *389*, 93–109.
32. Every, A.L.; Ng, G.Z.; Skene, C.D.; Harbour, S.N.; Walduck, A.K.; McGuckin, M.A.; Sutton, P. Localized suppression of inflammation at sites of *helicobacter pylori* colonization. *Infect. Immun.* **2011**, *79*, 4186–4192.
33. Chionh, Y.T.; Walduck, A.K.; Mitchell, H.M.; Sutton, P. A comparison of glycan expression and adhesion of mouse-adapted strains and clinical isolates of *Helicobacter pylori*. *FEMS Immunol. Med. Microbiol.* **2009**, *57*, 25–31.
34. Atkinson, S.C.; Dogovski, C.; Downton, M.T.; Pearce, F.G.; Reboul, C.F.; Buckle, A.M.; Gerrard, J.A.; Dobson, R.C.; Wagner, J.; Perugini, M.A. Crystal, solution and in silico structural studies of dihydrodipicolinate synthase from the common grapevine. *PLoS One* **2012**, *7*, e38318.

## Appendix

**Figure A1.** SPR analysis of 4A-1 V<sub>NAR</sub>. Binding of 4A-1 V<sub>NAR</sub> protein to immobilized 5G8 IgG (1450 RU) was analyzed at a constant flow rate of 50  $\mu\text{L}/\text{min}$  with an injection volume of 50  $\mu\text{L}$ . Injected concentrations were 8, 4, 2, 1 and 0.5  $\mu\text{M}$ . No regeneration was required between injection cycles as the bound 4A-1 V<sub>NAR</sub> completely dissociated within 300 s in the running buffer. Binding data (black lines, in triplicate) were fitted globally with a 1:1 kinetic interaction model (red lines) yielding a  $k_a$  of  $2.4 \times 10^4 \text{ M}^{-1}\text{s}^{-1}$ , a  $k_d$  of  $0.04 \text{ s}^{-1}$  and an equilibrium dissociation constant ( $K_D$ ) of 1.7  $\mu\text{M}$ . SensiQ Pioneer instrument docked with COOH1 chip was utilized for this measurement.

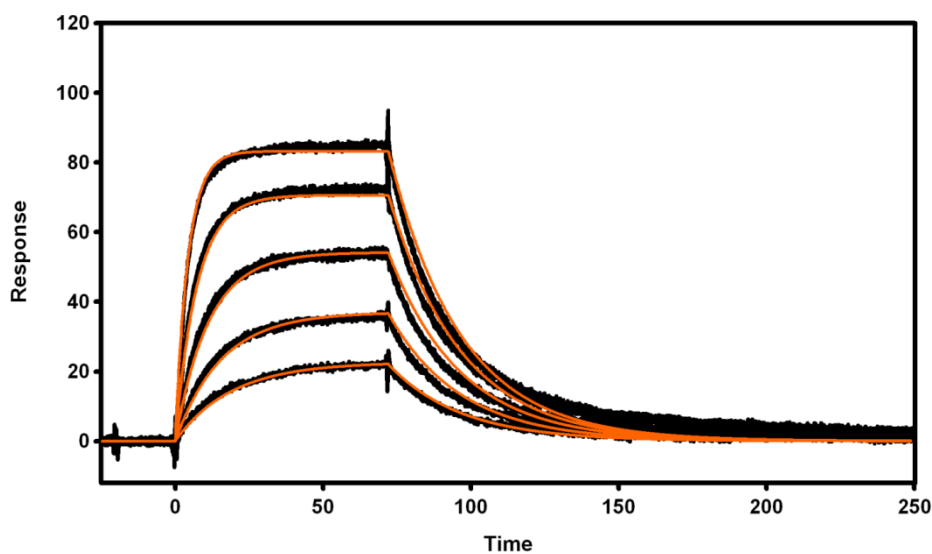


**Figure A2.** SPR analysis of the interaction between AMA-1 3D7 protein and 1F9 IgG. Approximately 185 RU of 1F9 IgG was captured onto an SPR chip via rabbit anti-mouse IgG at the start of each binding cycle. AMA-1 protein was injected at 50  $\mu\text{L}/\text{min}$  for 2 min and the dissociation monitored for either 300 s or 900 s. Injected AMA-1 concentrations were 729, 243, 81, 9 and 3 nM. Following dissociation phase, chip surface was regenerated with 10 mM Glycine pH 1.7 resulting in a complete removal of both AMA-1 and 1F9 proteins. Binding data (black lines, in duplicate) were fitted globally with a 1:1 kinetic interaction model (red lines) yielding a  $k_a$  of  $3.8 \times 10^4 \text{ M}^{-1}\text{s}^{-1}$ , a  $k_d$  of  $3.5 \times 10^{-5} \text{ M s}^{-1}$  and an equilibrium dissociation constant ( $K_D$ ) of 0.95 nM. SensiQ Pioneer instrument docked with COOH5 chip was utilized for this experiment.

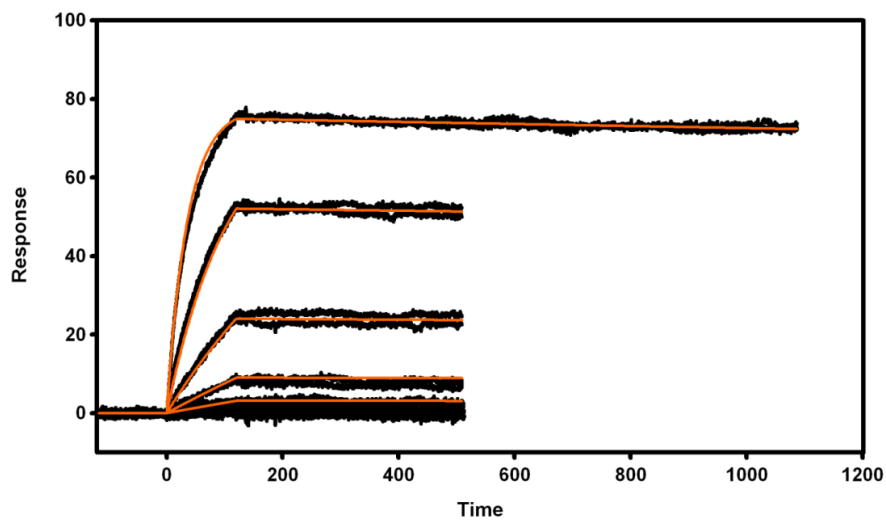


**Figure A3.** Retention of active  $V_{\text{NARS}}$  12Y-2 and 1411M-15, and mAbs 5G8 and 1F9 following heating at 60  $^{\circ}\text{C}$  in (a) liquid and (b) lyophilized formats, as determined by biosensor analysis. Method described in Section 3.3.3.

